ACS BIO & MED CHEM Au
AN OPEN ACCESS JOURNAL OF THE AMERICAN CHEMICAL SOCIETY

pubs.acs.org/biomedchemau
Article

A Promiscuous rSAM Enzyme Enables Diverse Peptide Cross-linking

Karsten A. S. Eastman, Marcus C. Mifflin, Paul F. Oblad, Andrew G. Roberts, and Vahe Bandarian*

Cite This: ACS Bio Med Chem Au 2023, 3, 480–493
Read Online

ACCESS | Metrics & More | Article Recommendations | Supporting Information

ABSTRACT: Ribosomally produced and post-translationally modified polypeptides (RiPPs) are a diverse group of natural products that are processed by a variety of enzymes to their biologically relevant forms. PapB is a member of the radical *S*-adenosyl-L-methionine (rSAM) superfamily that introduces thioether cross-links between Cys and Asp residues in the PapA RiPP. We report that PapB has high tolerance for variations in the peptide substrate. Our results demonstrate that branched side chains in the thiol- and carboxylate-containing residues are processed and that lengthening of these groups to homocysteine and homoglutamate does not impair the ability of PapB to form thioether cross-links. Remarkably, the enzyme can even cross-link a peptide substrate where the native Asp carboxylate moiety is replaced with a tetrazole. We show that variations to residues embedded between the thiol- and carboxylate-containing residues are tolerated by PapB, as peptides containing both bulky (*e.g.*, Phe) and charged (*e.g.*, Lys) side chains in both natural L- and unnatural D-forms are efficiently cross-linked. Diastereomeric peptides bearing (2*S*,3*R*)- and (2*S*,3*S*)-methylaspartate are processed by PapB to form cyclic thioethers with markedly different rates, suggesting the enzymatic hydrogen atom abstraction event for the native Asp-containing substrate is diastereospecific. Finally, we synthesized two diastereomeric peptide substrates bearing *E*- and Z-configured *γ*,*δ*-dehydrohomoglutamate and show that PapB promotes addition of the deoxyadenosyl radical (dAdo•) instead of hydrogen atom abstraction. In the *Z*-configured *γ*,*δ*-dehydrohomoglutamate substrate, a fraction of the dAdo-adduct peptide is thioether cross-linked. In both cases, there is evidence for product inhibition of PapB, as the dAdo-adducts likely mimic the native transition state where dAdo• is poised to abstract a substrate hydrogen atom. Collectively, these findings provide critical insights into the arrangement of reacting species in the active site of the PapB, reveal unusual promiscuity, and highlight the potential of PapB as a tool in the development peptide therapeutics.

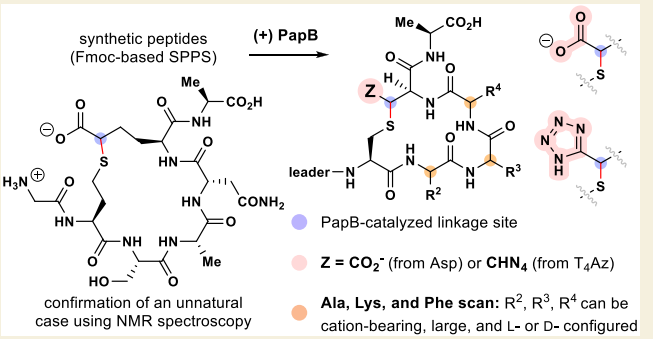

KEYWORDS: *peptide cross-linking, radical S-adenosyl-L-methionine, enzyme mechanism, RiPPs, radical chemistry*

INTRODUCTION

Enzymes have the remarkable ability to access and modify chemical space that would otherwise be inaccessible, making them of great interest in contemporary research.[1−3] However, the high substrate specificities that are a hallmark of enzymatic catalysis often necessitates directed modifications of the active site to achieve higher substrate tolerance at the expense of catalytic efficiency.[4−6] One growing class of enzymes that can functionalize unactivated carbon centers is the radical *S*-adenosyl-L-methionine (rSAM) superfamily, which catalyzes over 70 known reactions.[7] These enzymes contain one or more [Fe-S] clusters that coordinate to Cys thiolate side chains. The primary [4Fe-4S] cluster (RS) is coordinated to the enzyme by a universally conserved CXXXCXXC motif.[8,9] This cluster binds to the amino and carboxylate moieties of SAM via the unique Fe. Upon addition of a reductant, SAM is homolytically cleaved to form a deoxyadenosyl radical (dAdo•), which then abstracts an H-atom from the substrate to initiate a radical-mediated transformation (Scheme 1a).[9] Substrates for rSAM maturases include small molecules,[10−15] DNA,[16,17] RNA,[18−20] peptides,[21−27] and proteins.[28−30] However, regardless of the vast scope of both substrates and types of reactions catalyzed by rSAM maturases, few examples of harnessing their oxidative power to generalize bond formation at unactivated carbons exist.[31−35]

The rSAM enzyme PapB catalyzes the formation of six thioether cross-links between the Cys thiolate and C*β* of Asp residues located in a ribosomally synthesized and post-translationally modified polypeptide (RiPP) PapA.[36,37] The reaction is initiated by substrate H-atom abstraction (C*β* position) by dAdo• followed by cross-linking with the auxiliary cluster-ligated Cys thiolate concomitant with the reduction of the cluster to form the thioether cross-link (Scheme 1b).[37] In

Received: June 28, 2023
Revised: July 31, 2023
Accepted: August 1, 2023
Published: August 15, 2023

Scheme 1. Thioether Cross-linking by PapB[a]

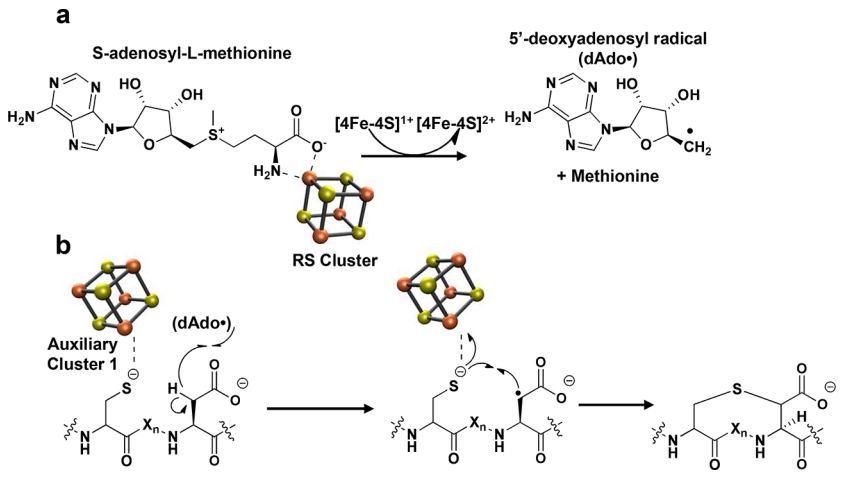

[a](a) Upon activation by an external reductant, SAM is homolytically cleaved to form 5′-dAdo• and Met. (b) dAdo•abstracts an H-atom from the peptide substrate and the radical is resolved via thioether formation and reduction of the auxiliary cluster.

our previous report, we demonstrated that PapB will cyclize Cys and Asp side chains that are adjacent as well as those separated by up to six residues.[35] Epimeric peptide substrates bearing D-configured Cys and Asp residues are also suitable for cyclization by PapB. Leveraging this tolerance, we generated a thioether containing analog of the FDA-approved drug octreotide, with a Cys-Glu cross-link replacing the disulfide in a threonine capped peptide. While this provided support for the use of rSAM maturases as biotechnological tools, several key demonstrations of substrate tolerance were lacking—namely, alterations of the donor and acceptor residues beyond D-amino acids, confirmation of what residues or side chain properties are tolerated at each position between donor and acceptor, and whether moiety isosteres of the donor or acceptor residues would be cross-linked.

In this study, we show that PapB can tolerate both side chain branching and extension, as well as modified substrates where each X in the CX_3D motif is systematically replaced with L- and D-forms of bulky (*e.g.*, Phe) and charged (*e.g.*, Lys) residues. We observe the unusual accommodation and cross-linking of a pharmaceutically relevant isostere of the carboxylate moiety, further highlighting the promiscuity of PapB. The ability to cross-link to extended carboxylate side chain containing amino acids led to the design and synthesis of unsaturated substrate analogs, which serve as mechanism-based inhibitors of enzyme turnover. The differential fates of the two diastereomeric peptide substrates provide molecular-level evidence for the arrangement of SAM and the thioether forming Cys in the active site of PapB. This research provides extensive evidence supporting the utility of PapB as a simple and predictable chemical biology tool to generate cross-linked peptides with highly variable physiochemical properties.

RESULTS

PapB Tolerates Side Chain Branches in Thiol- and Carboxylate-Containing Residues

PapB was overexpressed in *E. coli*, purified under anoxic conditions to homogeneity, and reconstituted with iron and inorganic sulfide (see Figure S1). Consistent with previously published results, using the minimal substrate (msPapA), the formation of a thioether cross-link between a Cys thiolate and Cβ of an Asp residue side chain in the same peptide is apparent by LC−MS (Figure S2a,b).[37] Treatment of msPapA with PapB produces a peptide product that is 2 Da lighter than the unmodified substrate, resulting from the loss of one hydrogen from the Cys thiol and another from Cβ of the Asp side chain. Mass spectrometry (MS) analysis shows a 2 Da change in the m/z of the monoisotopic peak in the product as compared to the assay without PapB (Figure S2c,d). A detailed tandem mass spectrometry (MS/MS) analysis of the cross-linked msPapA has been published previously;[35] as with previous reports on PapB using msPapA, the enzyme used below is highly active,[35] as evidenced by control experiments with msPapA that show quantitative conversion of peptide when incubated with PapB in 100-fold excess over the concentration of enzyme over a 15 min incubation (Figure S2).

Previous studies have shown that PapB will tolerate msPapA analogs where the Cys and Asp residues are adjacent as well as those separated by up to six residues.[35] In this effort, we first investigated the ability of PapB to tolerate modifications of the thiol- and carboxylate-containing residues. All the peptides used in these studies, including those with unnatural amino acids, were synthesized by Fmoc-based solid phase peptide synthesis (SPPS). The leader sequence in each peptide described is LKQINVIAGVKEPIRAYG. Unless otherwise indicated, the assays contained 0.2 mM of peptide (assessed by dry weight or Trp absorbance where present), which was incubated with 1.9 μM PapB, 2 mM SAM, and 2 mM sodium dithionite (NaDT), in a buffer solution containing 50 mM PIPES•KOH (pH 7.4), 300 mM KCl, 2 mM dithiothreitol (DTT) and 15% glycerol. Assays were quenched with trichloroacetic acid (TCA) 15 min after initiating the reaction with PapB (see the Materials and Methods section for details). The percent turnover in each assay was determined by comparison to simulated envelopes, as described in the Materials and Methods section.

To explore the ability of PapB to process unnatural amino acids with branched side chains, we incorporated penicillamine (Pen) or β-methylaspartate (Me-Asp) into the msPapA sequence. Penicillamine is an analog of Cys where two methyl groups replace the hydrogens at the Cβ of the side chain, whereas Me-Asp has a single methyl group on Cβ. PapB cross-links Pen-containing peptides (see Figure 1a, C19Pen msPapA,

https://doi.org/10.1021/acsbiomedchemau.3c00043
ACS Bio Med Chem Au 2023, 3, 480−493

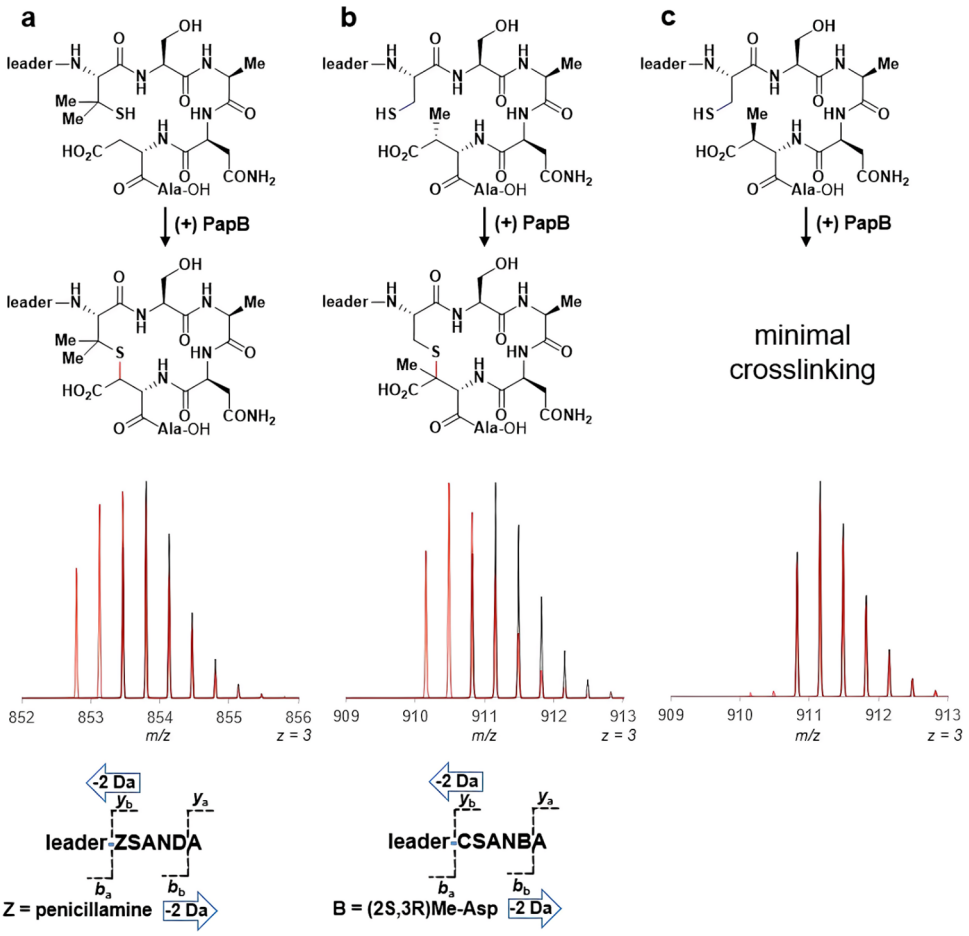

Figure 1. PapB cross-links branched amino acids. The leader sequence in each peptide described is LKQINVIAGVKEPIRAYG. (a) C19Pen containing msPapA is processed by PapB. A 2 Da loss is clearly seen in the MS. Partial alkylation is observed when reacted IAM due to the reaction not going to completion (Figure S4). See Figure S5 for MS/MS and all found fragments for C10Pen. (b) D23(2*S*,3*R*)Me-Asp containing msPapA is quantitatively cross-linked in 15 min by PapB. No alkylation of any free thiols is observed when reacted with IAM (Figure S4). (c) D23(2*S*,3*S*)Me-Asp containing msPapA is inefficiently processed by PapB. The small peaks that correspond to a 2 Da loss in the MS may be due to a contaminating diastereomer or from potential misalignments in the active site that still allow for H-atom abstraction to occur at a suboptimal location. Extended reaction times demonstrate that D23(2*S*,3*S*)Me-Asp msPapA will cross-link, albeit slowly (Figure S3). See Figures S6 and S7 for MS/MS and all found fragments of the D23(2*S*,3*R*)Me-Asp and D23(2*S*,3*S*)Me-Asp peptides respectively.

reacted species shown in red), albeit not as efficiently as msPapA, but still demonstrating that branched carbons on the thiol-containing side chain are tolerated by the enzyme. In the 15 min incubation, ∼30−40% conversion is observed, as evidenced by the ratio of the monoisotopic masses of the cross-linked versus unprocessed peptide (unmodified $[M + 3H]^{3+}$ calcd. 853.4635, found = 853.4656, ppm error = 2.46; modified $[M + 3H]^{3+}$ − 2 Da calcd. 852.7916, found = 852.7922, ppm error = 0.70).

Crystal structures of radical SAM enzymes, where available, show that the H-atom that is abstracted is generally within van der Waals distance of the site of dAdo• generation in the active site.[13,14,38−40] This suggests that RS enzymes would show preferences toward substrates that maintain an H-atom with appropriate distance from the site of generation of the dAdo•. We reasoned that the differing orientations of the methyl substituent at the Cβ of Me-Asp would lead to distinct cross-linking activities by PapB. Any preference for one diastereomeric substrate to cyclize would illuminate which of the native prochiral β-hydrogen atoms of Asp (D23) is abstracted. Me-Asp containing peptides incorporating either (2*S*,3*R*)-2-amino-3-methylsuccinic acid [(2*S*,3*R*)Me-Asp] or (2*S*,3*S*)-2-amino-3-methylsuccinic acid [(2*S*,3*S*)Me-Asp] in place of D23 were synthesized and incubated with PapB. An *N*-terminal Trp residue was added to ensure accurate quantitation of the concentrations of the two enantiomers being tested. D23-(2*S*,3*R*)Me-Asp is cross-linked by the enzyme efficiently (Figure 1b; unmodified $[M + 3H]^{3+}$ calcd. 910.8180, found = 910.8176, ppm error = −0.44; modified $[M + 3H]^{3+}$ −2 Da calcd. 910.1462, found = 910.1467, ppm error = 0.55). As with the wildtype substrate, complete cross-linking is observed with this epimer. By contrast, the D23(2*S*,3*S*)Me-Asp peptide exhibits little to no cross-linking in the 15 min timeframe (Figure 1c). The small quantities of observed cross-linked product may be the result of a diastereomeric impurity (*e.g.*, D23(2*S*,3*R*)Me-Asp) introduced from the commercial residue. These results are significant, as they allow one to assign the *Pro-S* hydrogen at the Cβ of the amino acid as the preferred site of H-atom transfer in the native D23-containing substrate. We note that when incubated for extended periods (18 h), the D23(2*S*,3*S*)Me-Asp-containing substrate msPapB analog does show ∼70% cross-linking when comparing the ratios of monoisotopic masses (see Figure S3, modified $[M + 3H]^{3+}$ − 2 Da calcd. 910.1462, found = 910.1503, ppm error = 4.50).

https://doi.org/10.1021/acsbiomedchemau.3c00043
ACS Bio Med Chem Au 2023, 3, 480−493

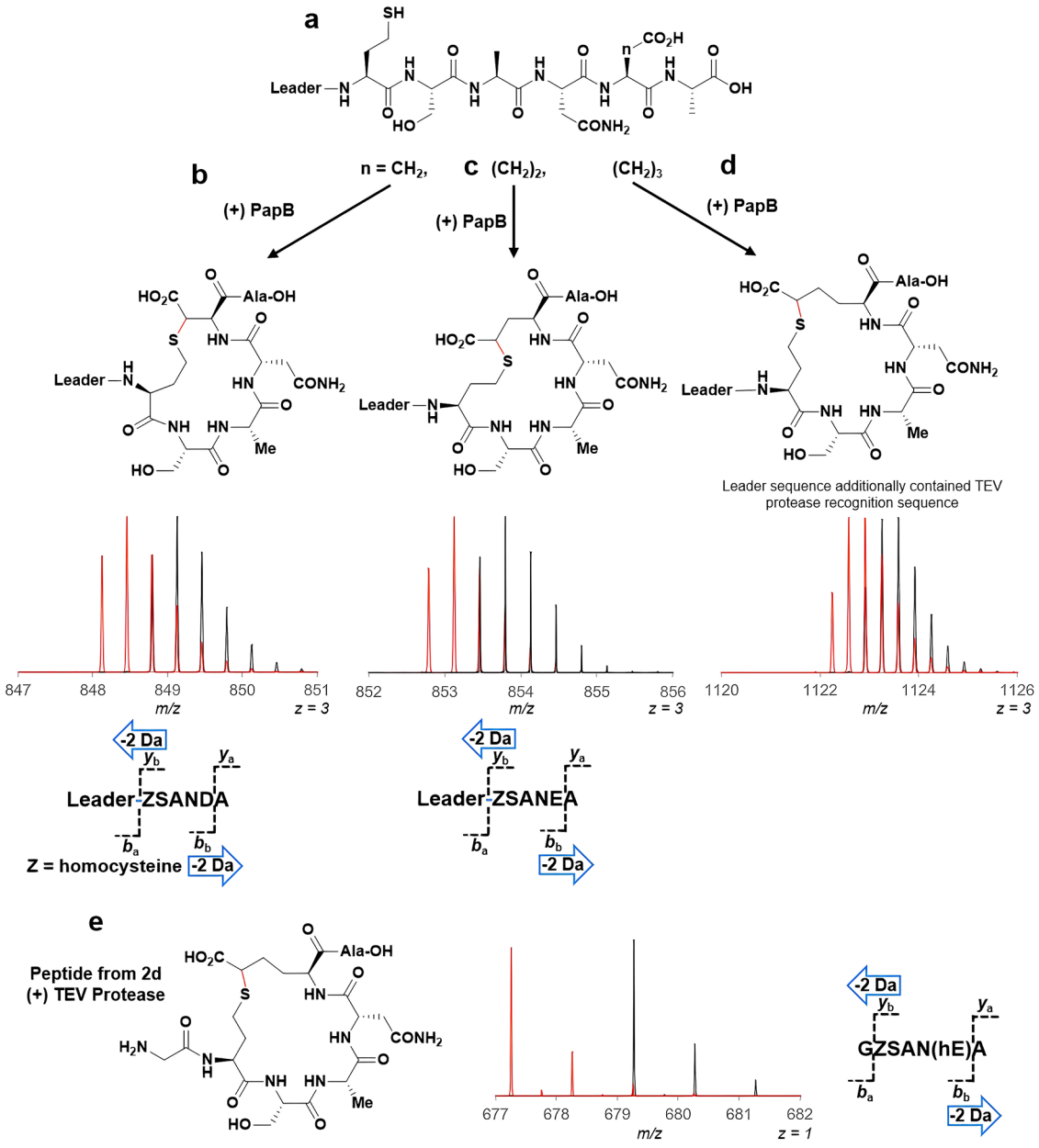

Figure 2. PapB forms cross-links in extended thiol- and carboxylate-containing side chains. (a) A generalized linear C19hCys msPapA is shown—where n = CH_2 (Asp), $(CH_2)_2$ (Glu), or $(CH_2)_3$ (hGlu). (b) When the carboxylate-containing residue is Asp, a Δ2 Da change is clearly seen in the MS. MS/MS shows no fragments found between the hCys and Asp (Figure S9). (c) When the carboxylate-containing residue is Glu, a Δ2 Da change is clearly seen in the MS. There are no fragments between hCys and Gly in the MS/MS (Figure S10). (d) PapB cross-links an msPapA peptide containing both hCys and hGlu. Using a sequence of Leader-ENLYFQG[hCyc]SAN[hGlu]A, which contains a TEV protease recognition sequence, we first reacted the peptide with PapB. (e) Peptide from panel (d) was reacted with TEV protease to liberate a macrocyclized peptide core from the leader sequence. See Figure S11 for all fragments found in the MS/MS of this macrocycle and Figures S12 and S13 for the linear and cyclized peptide ^{1}H NMR confirming regiochemistry of the cross-link. Peptide controls are shown in black whereas the red spectra reflect addition of PapB.

We cannot exclude that there are sufficient rotational degrees of freedom in the active site that would support placing the *Pro-R* H-atom within the vicinity of the generated dAdo•, though the >100-fold rate difference for the D23(2*S*,3*R*)Me-Asp versus the D23(2*S*,3*S*)Me-Asp diastereomer suggests a preference for the *Pro-S* H-atom. We also cannot exclude the possibility that some of the (2*S*,3*S*) isomer racemizes in the 18 h incubation. Nevertheless, to confirm that in each of the cases above, PapB still catalyzes the formation of a thioether cross-link and that the alternate amino acids do not lead to altered regiochemical outcomes, each of the reaction mixtures was subjected to iodoacetamide (IAM) treatment after reaction with PapB. No carbamidomethylation is seen in peptides that show full conversion, such as the D23(2*S*,3*R*)Me-Asp-msPapA (Figure S4). By contrast, partial carbamidomethylation is seen in the C19Pen scenario because the reaction did not go to completion (Figure S4) and the unreacted peptide bears a thiol moiety. At the 18 h timepoint, the D23(2*S*,3*S*)Me-Asp peptide still shows carbamidomethylatation due to inefficient PapB processing of that variant (Figure S4). The modified peptides were additionally subjected to MS/MS. Both the C19Pen and D23(2*S*,3*S*)Me-Asp msPapA variants show fragments between

https://doi.org/10.1021/acsbiomedchemau.3c00043
ACS Bio Med Chem Au 2023, 3, 480−493

the donor and acceptor residues because a portion of the substrate did not go to completion; these *y*- and *b*-ions act as an internal standard to demonstrate unmodified peptide fragments between each residue. A 2 Da loss is observed in *b*-ions generated by peptide bond fragmentation C-terminal to the carboxylate-containing residue a 2 Da loss is observed in *y*-ions generated by peptide bond cleavage N-terminal to the thiol-containing residue (see Figures S5 and S6 for full MS/MS spectra and all found fragments for the C19Pen and D23(2*S*,3*S*)Me-Asp peptides, respectively). As with the wildtype substrate, no *b*- or *y*-ions were observed between the thiol- and carboxylate-containing residues in the D23-(2*S*,3*R*)Me-Asp variant. The D23(2*S*,3*R*)Me-Asp variant shows a 2 Da loss in the *b*-ions after the Me-Asp residue and in the *y*-ions after the Cys residue. See Figure S7 for full MS/MS spectra and all fragments found for D23(2*S*,3*R*)Me-Asp peptide.

Taken together, these results demonstrate that PapB is tolerant of side chain branches in thiol-containing residues and prefers *Pro-S*-configured H-atom abstraction in the native Asp residue. These findings support our previous hypothesis that the thiol at Cys and the carboxylate at Asp or Glu residues are critical moieties necessary for substrate recognition and processing by PapB. The selectivity associated with the Me-Asp residues is suggestive that dAdo• preferentially abstracts the *Pro-S* hydrogen of the native substrate.

PapB Cross-links Extended Side Chains of Thiol- and Carboxylate-Containing Residues

Previous studies have demonstrated that PapB can tolerate extended side chains of the acidic residue, as both CXXXD and CXXXE sequences are cross-linked.[37] Here, we provide evidence that PapB can form cross-links in msPapA with a homocysteine (hCys, Figure 1a) substitution at position 19 and an Asp in position 23 (Figure 2b), C19hCys and D23E (Figure 2c), and C19hCys and homoglutamate (hGlu) at position 23 (Figure 2d). The MS analyses of the reaction products show that each substrate undergoes cross-linking, as evidenced by a 2 Da loss relative to the substrate due to the loss of one H from the hCys thiol and a second H from carboxylate-containing residue at position 23. Remarkably, PapB catalyzes formation of a cross-link in peptides containing hCys at position 19 and Asp (unmodified $[M + 3H]^{3+}$ calcd. 848.7916, found = 848.7895, ppm error = −2.47; modified $[M + 3H]^{3+} - 2$ Da calcd. 848.1197, found = 848.1215, ppm error = 2.12), C19hCys and D23E (unmodified $[M + 3H]^{3+}$ calcd. 853.4635, found = 853.4600, ppm error = −4.10; modified $[M + 3H]^{3+} - 2$ Da calcd. 852.7916, found = 852.7926, ppm error = 1.17), or C19hCys D23hGlu at position 23 with a modified leader sequence containing a TEV protease cleavage site (unmodified $[M + 3]^{3+}$ calcd. 1122.9220, found = 1122.9233, ppm error = 1.16; modified $[M + 3]^{3+} - 2$ Da calcd. 1122.2501, found = 1122.2487, ppm error = −1.25). As a proof of concept for the use of PapB in generating macrocyclic peptides, the C19hCys/D23hGlu variant with a TEV cleavage site could be cleaved with the protease to generate a macrocyclic peptide (Figure 2e). Our previous results demonstrated that changing the donor and/or acceptor amino acid to the D-variant resulted in cross-linking, albeit at a reduced efficiency compared to the results in Figure 2. To confirm that the cross-linking involves formation of a thioether, peptides cross-linked under these conditions do not undergo carbamidomethylation when treated with IAM (Figure S8). The regiochemistry was further confirmed by MS/MS, which reveals no *b*- or *y*-ions between the thiol- or carboxylate-containing residues, indicating the formation of a stable non-alpha thioether linkage. As with all previous results of cross-linked peptides by PapB, a 2 Da loss is observed in the *b*-ions C-terminal to the carboxylate-containing residue and a 2 Da loss is observed in all *y*-ions N-terminal to the hCys residue. The MS/MS spectra and observed ions for C19hCys are shown in Figure S9, for C19hCys/D23E in Figure S10, and for TEV-cleaved C19hCys/D23hGlu in Figure S11.

The observation of a 2 Da shift, when taken together with the MS/MS data and the loss of the IAM-sensitivity clearly shows that a thioether cross-link has formed. However, we wanted to confirm that as with the wildtype substrate, the cross-link is to the carbon atom that is alpha to the carboxylate of the side chain. To this end, either unmodified or cross-linked C19hCys/D23hGlu was treated with TEV protease to liberate the core from the leader peptide, purified by HPLC, and subjected to both one- and two-dimensional NMR spectroscopic analysis. The 1D NMR spectrum of the acyclic peptide, prior to the treatment with PapB, reveals a resonance at 2.40 ppm, which is composed of an apparent triplet of doublets integrating to two protons (Figure S12). We assign this feature to the geminal Cδ protons of hGlu. In the NMR spectrum of the cyclized peptide (Figure S13), the 2.40 ppm resonance is absent and a distinct triplet at 3.29 ppm integrating to one proton is observed. This 3.29 ppm resonance is consistent with thioether installation at the Cδ position, which is alpha to the carboxylate in the hGlu side chain. To further correlate connectivity, the acyclic and modified peptides were subjected to 2D rotating frame Overhauser enhancement spectroscopy (ROESY) analyses to establish through-space correlations of protons. In the acyclic peptide, the resonance at 2.40 ppm (hGlu, Cδ-H, 2H) is correlated to resonances at 1.65 ppm (hGlu, Cγ-H, 2H), 1.74 ppm (hGlu, Cβ-H), and 1.86 ppm (hGlu, Cβ-H), all of which are additionally correlated with 4.31 ppm (hGlu, Cα-H; indicating the anticipated through-space interactions for the hGlu side chain, see Figure S14). The acyclic hCys resonances at 2.63 ppm (hCys, Cγ-H), 2.56 ppm (hCys, Cγ-H), 2.05 (hCys, Cβ-H, 2H), and 4.58 ppm (hCys, Cα-H) are correlated but lack additional through-space interactions. In the modified peptide, the distinct resonance at 3.29 ppm (hGlu, Cδ-H, 1H) is correlated to resonances at 1.87 ppm (hGlu, Cγ-H, 2H), 1.92 ppm (hGlu, Cβ-H), and 1.96 ppm (hGlu, Cβ-H) (see Figure S15). The comparison of the acyclic and the cyclized (modified) peptide 1D spectra show a ppm shift ranging from 0.1−0.22 in the resonances between 1.6 and 2.0, which would make the coupled resonances in the modified peptide ROESY spectra consistent with a through-space coupling of Cδ-H of the hGlu side chain to Cγ-H and Cβ-H of hGlu. Additionally, the acyclic Cβ-H of hCys resonance at 2.05 shifts to 2.10 ppm, which is correlated with the >0.2 ppm shifted hCys Cγ-H at 2.56 and 2.63 ppm. Importantly, the Cδ-H of hGlu at 3.29 ppm is observed to have weak correlations with the hCys Cγ-H and Cβ-H resonances at 2.63, 2.56, and 2.10 ppm; these resonance-couplings are not present in the acyclic peptide. These cross peaks are consistent with cross-linking of the hCys thiol with the hGlu Cδ and demonstrate that PapB can cross-link extended side chains of thiol- and carboxylate-containing residues.

While various levels of promiscuity have been reported in the rSAM RiPP field, changing both the identity of both the

https://doi.org/10.1021/acsbiomedchemau.3c00043
ACS Bio Med Chem Au 2023, 3, 480−493

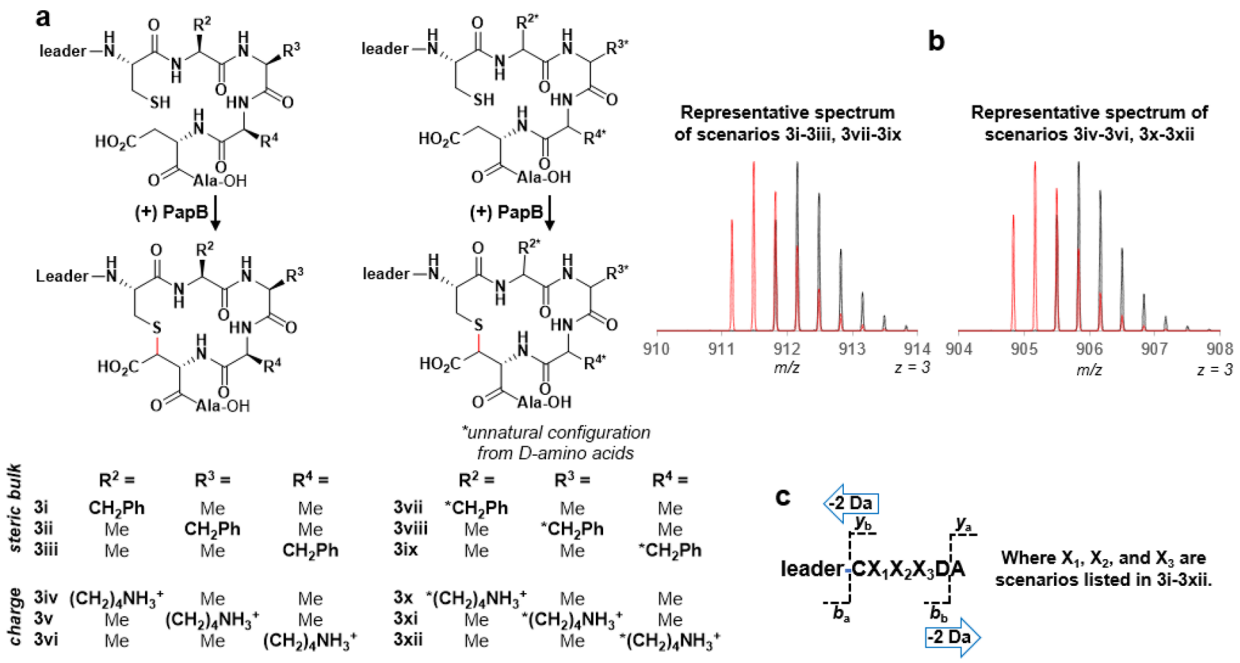

Figure 3. PapB forms thioether cross-links with bulky or charged residues at every intervening position. (a) General cross-linking schematic and each scenario for L- (left hand side of 3a) or D-amino acids (right hand side of 3a) that contain bulk or charge at each position between Cys and Asp. (b) Representative MS for each scenario—the generalized MS for motifs that contain L- or D-Phe is shown on the left whereas the generalized MS for motifs that contain L- or D-Lys is shown on the right. In all cases, a Δ2 Da shift is seen in the MS; compare unreacted (black) to reacted (red). See Figures S16−S19 for the individual MS of IAM-treated versions of both the PapB-processed and -unprocessed peptides. (c) Tandem mass spectrometry for scenarios 3i-3xii show no fragmentation between the Cys and Asp. A 2 Da loss is present in every *y*-fragment C-terminal to the Cys and the *b*-fragments N-terminal to the Asp. Figures S20−S31 show the MS/MS spectra and fragments found for each respective unreacted and reacted peptide.

donor and acceptor residues and forming a chemically consistent product is unprecedented. These findings expand our understanding of the capabilities of PapB and have implications for the novel biosynthesis of RiPPs that contain modified and unnatural side chains.

Cross-linking of CXXXD Motifs with Bulky and Charged Residues

The flexibility of PapB in processing variants of msPapA where the residues between the thiol- and carboxylate-containing residues in the cross-linking reaction was explored by systematically replacing X_1, X_2, and X_3 in the $CX_1X_2X_3D$ motif with L-Phe, D-Phe, L-Lys, and D-Lys. PapB effectively processes all CXXXD motifs variants that include bulky (represented by L-Phe and D-Phe) and charged (represented by L-Lys and D-Lys) residues at the intervening positions; an N-terminal Trp was included for each variant to allow for accurate quantification of substrates. Representative figures and MS data for cross-linking of $X_1X_2X_3D$ where X_1, X_2, and X_3 are systematically replaced with L-Phe, D-Phe, L-Lys, and D-Lys are depicted in Figure 3. For each variant, a 2 Da loss is observed in the MS (see Figure 3b for representative spectra in the Phe and Lys-containing series). In all PapB-processed samples that contain the presumed thioester linkage, treatment with IAM leads to no carbamidomethylation, corroborating the absence of a reactive thiol moiety (see Figures S16−S19 for each $X_1X_2X_3D$ variant ± PapB and subsequent IAM treatment and ppm error for each variant ± PapB). Finally, no fragmentation is observed between the Cys and Asp residues by MS/MS (Figure 3c shows the general schematic), which is also consistent with a cross-link forming between these residues. Moreover, a 2 Da loss is observed in all the *b*-ions C-terminal to the Asp residue and in every *y*-ion N-terminal to the Cys residue. As a control, a separate set of each unmodified peptide also underwent MS/MS to demonstrate the positional differences of the varied amino acid residues. For a direct comparison of the MS/MS spectra and all fragments found for each reacted and unreacted scenario, see Figures S20−S22 for the L-Phe variants, Figures S23−S25 for the L-Lys variants, Figures S26−S28 for the D-Phe variants, and Figures S29−S31 for the D-Lys variants.

The results presented in this section show remarkable pliability of the active site of PapB, which can process a wide range of structurally diverse substrates. Although there are few demonstrated cases,[41] the ability of any native enzyme to tolerate such flexibility is uncommon and highlights the robustness of the system.

Cross-linking to a Tetrazole-Containing Side Chain: Implications for Peptide-Based Therapeutics

While the data with hCys, hGlu, and D-amino acid containing peptides all suggest a high level of tolerance in PapB for various substrates, the examples shown are limited by the fact that they all contain a thiol- and carboxylate-containing residue. We have demonstrated that selenocysteine peptides are processed by PapB,[42] but as far as we are aware, no examples of an isostere of a carboxylate moiety being processed by an rSAM RiPP maturase are known. Tetrazole moieties are commonly used as bioisosteric replacements for carboxylic acid moieties in small-molecule drug development. Tetrazole moieties can improve the bioavailability of drugs,[43] increase their lipophilicity,[44] and reduce side-effects when compared to carboxylate-containing compounds.[45] This is due to the metabolic stability of tetrazole moieties—metabolic transformations of carboxylic acids are

https://doi.org/10.1021/acsbiomedchemau.3c00043
ACS Bio Med Chem Au 2023, 3, 480−493

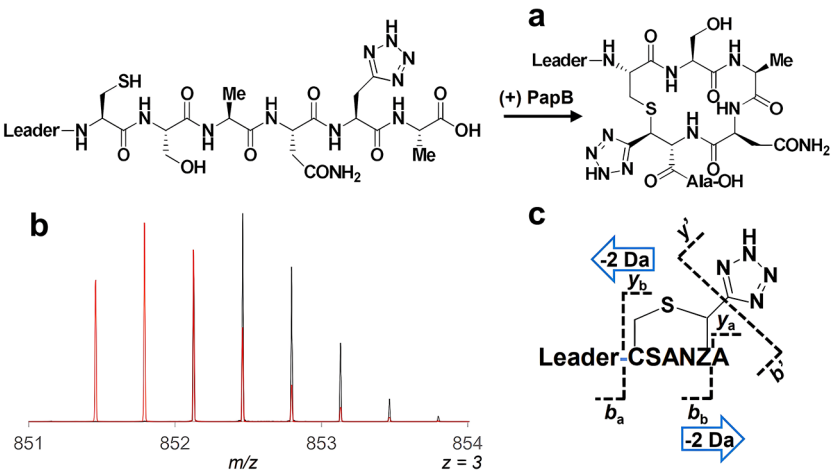

Figure 4. Carboxylate isostere (tetrazole moiety) is cross-linked by PapB. (a) Schematic of the linear and cyclized peptide shows the putative cross-link location. (b) MS results show a clear 2 Da loss between an assay without PapB (black) and with the addition of PapB (red). (c) Tandem mass spectrometry shows no fragmentation between Cys and T4Az (see Figure S33). Further, there is evidence in the MS/MS of fragmentation of the tetrazole moiety (y' and b'; see Figure S34).

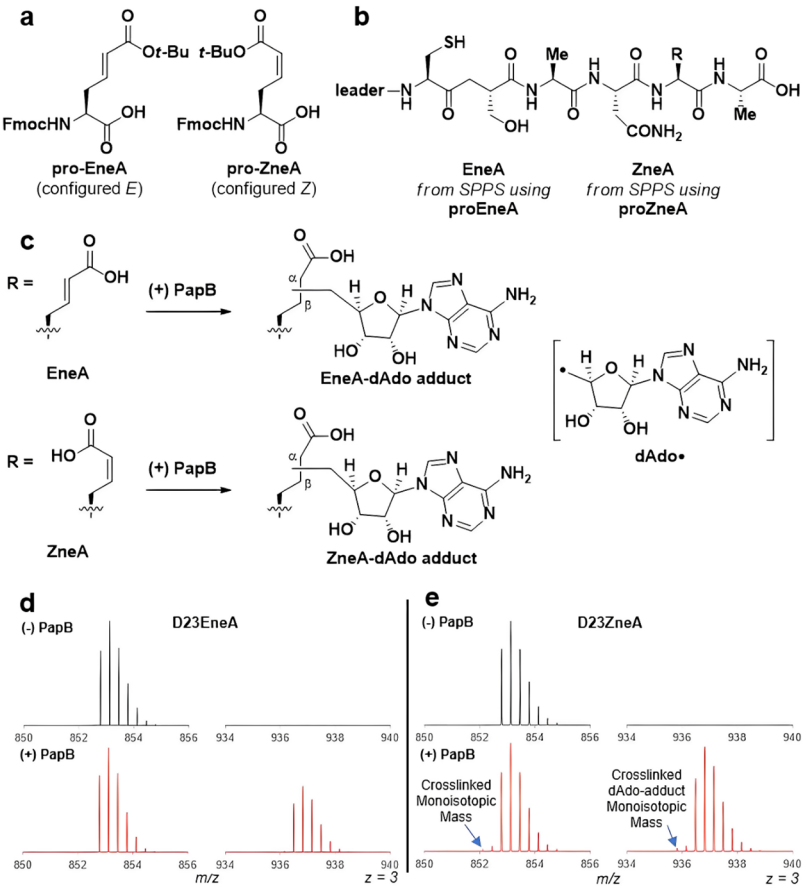

Figure 5. Analogs of hGlu (EneZ and ZneA) in msPapA are turned over by PapB. (a) EneA and ZneA are olefinic analogs of hGlu. (B) Linear, unreacted peptide sequence where R = EneA or ZneA is shown. (c) Upon addition of PapB, a dAdo adduct is observed in the MS. The adduct is localized to the EneA or ZneA residue through MS/MS (see Figures S42 and S43 for MS/MS of reacted EneA and ZneA respectively). The attachment site (α or β) was not determined. (d) Representative spectra of the D23EneA peptide are shown in the absence or presence of PapB. Addition of PapB shows a new isotopic envelope that is consistent with a dAdo adduct (calculated m/z = 936.4922, observed m/z = 936.4903, ppm error = −2.03). (e) As with D23EneA peptide, the D23ZneA peptide forms a deoxyadenosine adduct in the presence of PapB (observed m/z = 936.4915, ppm error = −0.75). However, in the spectra of peptide treated with PapB, there is also evidence of a cross-linked peptide both in the parent mass envelope (~3% turnover, expected m/z = 852.1191, observed m/z = 852.1203, ppm error = 1.41) and in the deoxyadenosine adduct mass envelope (~5% turnover, expected m/z = 935.8203, observed m/z = 935.8198, ppm error = −0.535). Upon addition of IAM, the free thiol in both the parent and dAdo-adduct is carbamidomethylated—however, the feature consistent with a *bona fide* thioether cross-link is not (see Figure S44).

https://doi.org/10.1021/acsbiomedchemau.3c00043
ACS Bio Med Chem Au 2023, 3, 480−493

driven in part by microsomes of the liver,[46] many of which are evaded with a tetrazole isostere.[47] The tetrazole pharmacophore has been used in a variety of drug classes, including nonsteroidal anti-inflammatory drugs,[48] angiotensin receptor blockers,[49] and as broad spectrum antibiotics.[50]

To determine if the carboxylate-containing amino acid of msPapA can be replaced with the isosteric tetrazole-containing amino acid, we incorporated (2*H*-tetrazol-5-yl)propanoic acid (T4Az) into msPapA (D23T4Az) by SPPS (using commercial (*S*)-2-(Fmoc-Amino)-3-(1*H*-tetrazole-5-yl)propanoic acid) CAS 954147-35-4) and incubated the resultant peptide with PapB. The structures of the linear and cyclized peptides are shown in Figure 4a. Upon reaction with PapB, a 2 Da shift is clearly observed (Figure 4b; (unmodified $[M + 3H]^{3+}$ calcd. 852.1272, found = 852.1269, ppm error = −0.35; modified $[M + 3H]^{3+}$ −2 Da calcd. 851.4553, found = 851.4550, ppm error = −0.35), suggesting formation of a cross-link. Addition of IAM does not lead to carbamidomethylated species, consistent with complete processing of the thiol moiety (Figure S32). The MS/MS spectra of D23T4Az msPapA reveals no fragmentation between the Cys and T4Az residue (Figure 4c), but the anticipated 2 Da loss is observed in the *b*-ions C-terminal to the T4Az residue, and in the *y*-ions N-terminal to the Cys residue (see Figure S33 for the MS/MS spectra and all found fragments). While we do not know the regiochemistry for the cross-link, several unusual peaks are present in the MS/MS that are potentially informative. For example, we observe peaks (Figure 4c,*y*′ and *b*′) that are consistent with loss of the tetrazole moiety (see also Table S1 for additional *y*′- and *b*′-fragments). While not unambiguous, these fragments suggest that the thioether forms alpha to the tetrazole. Interestingly, incubation of D23H msPapA did not lead to any cross-linking (Figure S34), further supporting a role for the tetrazole as a carboxylate-moiety isostere in PapB.

This data with the tetrazole analog is the first-demonstrated ability of rSAM RiPP maturases to cross-link a carboxylate isostere, opening new avenues for the development of peptide-based therapeutics. By using the tetrazole moiety in place of a carboxylate, the metabolic stability and pharmacokinetic properties of potential peptide therapeutics can be improved. This finding greatly expands the scope of rSAM RiPP maturases.

Unsaturated Peptide Side Chains Reveal a Transition State Analog

The ability of PapB to cross-link peptides containing hGlu presents a rare opportunity to probe the aspects of the radical-mediated transformation using unsaturated analogs. The *N*-Fmoc and side chain carboxylate ^{t}Bu ester protected *E- and Z*-configured L-*γ*,*δ*-dehydrohomoglutamate analogues (proEneA and proZneA, Figure 5a) were synthesized by olefin cross metathesis of allyl glycine derivatives.[51] Each diastereomeric residue was incorporated in place of msPapA D23 position using SPPS (Figure 5b). See Figure S35 for the synthetic scheme of proEneA and proZneA, Figures S36 and S37 for the ^{1}H and ^{13}C NMR of proEneA, Figure S38 for the HPLC−MS characterization of proEneA, Figures S39 and S40 for the ^{1}H and ^{13}C NMR of proZneA, and Figure S41 for the HPLC−MS characterization of proZneA. Each diastereomeric residue was incorporated in place of D23 in msPapA by SPPS to give (*S*,*E*)-5-aminohex-2-enedioic acid (EneA) and (*S*,*Z*)-5-aminohex-2-enedioic acid (ZneA) peptides (Figure 5b).

Incubation of D23EneA or D23ZneA msPapA variants with PapB leads to formation of several products. In both cases, we observe formation of a peptide-dAdo adduct, as evidenced by the formation of a peak with *m*/*z* of 936.4922 (see Figure 5c−e; [dAdo-adduct $[M + 3H]^{3+}$ calcd. 936.4922, found = 936.4920 (D23EneA), ppm error = −0.21 (D23EneA); found = 936.4911 (D23ZneA), ppm error = −1.17 (D23ZneA)]. MS/MS analysis of each product localizes the dAdo-adduct to the olefinic amino acid analog (see Figures S42 and S43 for all found fragments of the EneA and ZneA msPapA variants). Careful analysis of the MS data show that a small portion of the ZneA containing peptide, in addition to being modified with dAdo, also undergoes a 2 Da mass loss, which is consistent with the formation of a thioether cross-link (Figure 5e; dAdo-adduct thioether $[M + 3H]^{3+}$ calcd. 935.0823, found = 935.0831, ppm error = 0.86). Additionally, approximately 5% of the ZneA peptide also shows a 2 Da loss in the parent envelope, suggesting formation of a cross-link but no dAdo adduct formation (Figure 5e, parent peak unmodified $[M + 3H]^{3+}$ calcd. 852.7916, found = 852.7879, ppm error = −4.33 parent peak modified −2 Da $[M + 3]^{3+}$ calcd. 852.1197, found = 852.1203, ppm error = 0.70).

To further confirm that the 2 Da loss observed corresponds to thioether cross-link formation, reaction products were subjected to IAM treatment. Addition of IAM to the unmodified portion ZneA and EneA peptides results in carbamidomethylation of the free thiol (Figure S44). However, the species corresponding to the envelopes showing a 2 Da loss do not show further modification in the presence of IAM, regardless of whether they are additionally modified by dAdo. MS/MS analysis of the species showing the 2 Da loss further confirmed regiochemistry of the cross-link (Cys to ZneA; see Figure S45). The apparent thioether cross-linking of ZneA is observed in two ways; a portion of the dAdoH-peptide adduct that contains a 2 Da loss does not appear to carbamidomethylate upon addition of IAM, and both the parent peak and the dAdo-adduct peak demonstrate a pattern in MS/MS that is consistent with the C19Pen scenario—a 2 Da loss is seen in *b*-fragments C-terminal to the ZneA residue, and a 2 Da loss is seen in the *y*-fragments N-terminal to the Cys residue. However, because it did not fully cross-link, a portion of the peptide acts as an internal control (see Figures S45 and S46 for all found fragments of the cross-linked parent peak and the cross-linked dAdo-adduct peak).

These scenarios show differences in the reactivity of the unsaturated carbons in these substrates when reacted with PapB, likely stemming from differences in how they are bound in the active site. The olefin introduces a strong preference, in the case of the EneA containing amino acid, for the carbon that would normally be attached to the sulfur of the Cys residue being placed too far from the site of reactivity. In the case of EneA, dAdo-addition to the substrate followed by quenching of the resulting radical intermediate leads to a dAdo-modified peptide with no evidence for cross-linking. In the case of ZneA, a significant fraction of the peptide has the same fate (dAdo-adduct formation but no cross-linking). Our interpretation of the fraction of the peptide that is both cross-linked and modified by dAdo is that the initial dAdo addition is to the carbon beta to the carboxylate, which would then generate a resonance-stabilized radical alpha to the carboxylate—this scenario is reminiscent of the hypothesized mechanism for the native substrate where H-atom abstraction generates a resonance stabilized radical. This would position the radical

https://doi.org/10.1021/acsbiomedchemau.3c00043
ACS Bio Med Chem Au 2023, 3, 480−493

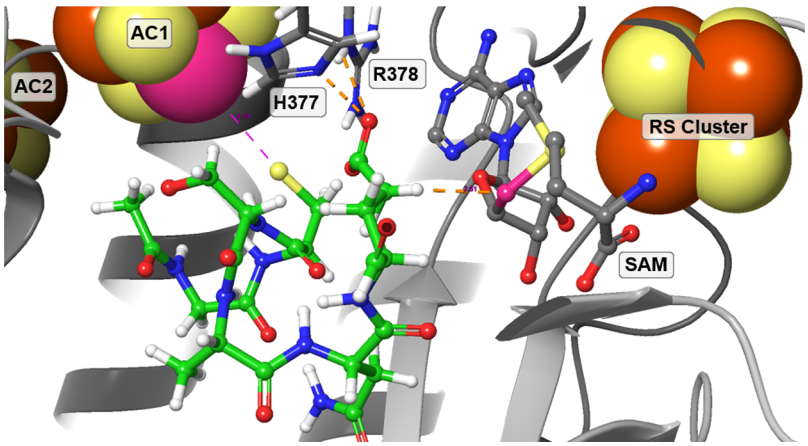

Figure 6. Predicted structure of PapB docked with a truncated, energy minimized form of msPapA. SAM and the peptide are shown to bind the RS cluster and Aux1, respectively. The peptide was manually docked into the structure, with the interaction between the coordinatively unsaturated Fe (shown in pink) and the thiol as the only constraint. The *Pro*-S hydrogen is connected with a dotted line to the 5′-carbon of SAM (shown in pink). Residues H377 and R378 appear in close proximity of the carboxylate of the cross-linking side chain, suggesting a role for these residues in amino acid specificity and binding.

in a position amenable to thioether cross-linking. The differential reactivity of ZneA and EneA analogs likely reflects the regiochemistry of the initially formed product, which in one case supports productive binding for thioether formation, and in the other case does not. At this point, we cannot rule out any alternative models in the case of ZneA where the initially formed dAdo adduct, which would still contain a radical intermediate, is sufficiently close to the Cys residue to permit formation of a thioether (see Figure S46).

In our studies of the dAdo adducts formed with either EneA or ZneA variants, we made an interesting observation that suggests that the adduct serves as a suicide or mechanism-based inactivator of the enzyme. All the experiments in this section utilized a 1:2 enzyme:peptide (40 μM:80 μM) ratio. In each case, when wild-type msPapA was added after 10 min of incubation with D23EneA or D23ZneA msPapA, minimal cross-linking was observed in the msPapA even after 18 h (Figure S47). This is unusual given that PapB is highly active, even a small amount of the enzyme can efficiently turnover msPapA. Indeed, when we set up the assays with enzyme concentration in excess of that of the EneA or ZneA peptide, or added PapB along with the msPapA, cross-linking of the msPapA was clearly observed (see Figure S48). While we cannot rule out that the ZneA or EneA containing peptides potentially bind the enzyme quite tightly, we note that the dAdo-adduct EneA/ZneA containing peptides mimic the ternary complex of the enzyme immediately after reductive cleavage of SAM. Taken together with the controls described above, a strong inference for the dAdo adducts serving as tight binding transition state analogs is plausible.

DISCUSSION

The central dogma that has guided enzymologists is that enzymes accelerate rates of reactions by binding through specific interactions and reducing the barrier toward the formation of products. Within any family of enzymes that catalyze a specific transformation, the physiological substrate specificity is achieved by evolutionary pressures that lead to multiple specific mutations that adapt the enzyme for a particular substrate, without compromising catalytic efficiency. In the last several decades, these lessons have been implemented in the laboratory settings by directed evolution experiments that have been able to greatly expand the substrate and reaction scope of many enzymes, though often the expanded substrate scope is accompanied by altered catalytic efficiency.[52−55] In the context of catalysts, enzymes are unique in their ability to recognize specific structures, often through multiple interactions that are generally remote from the site of chemistry. By contrast, small molecular catalysts often function by specifically recognizing the reacting groups and effecting their transformations. PapB appears to have the properties of both an enzymatic catalyst and a generalized catalyst for introduction of thioether bonds into peptides containing a thiolate and a carboxylate-like moiety. Our studies have uncovered a level of substrate promiscuity that challenges standard notions of enzyme specificity but also underscores the concept that while evolution has often achieved amazing specificity and catalytic efficiency, that outside of their cellular contexts, many enzymes involved in the production of rare natural products may be capable of much more than we observe *in vivo*. Evolutionary pressures in the cell may not have been so great as to reach the exquisite level of substrate specificity in these enzymes that we see in others, such as key housekeeping or metabolic enzymes. This may be particularly true in the context of RiPP maturase enzymes, where high substrate specificity from the leader sequence can be achieved distally from the active site, which may require only limited interactions for the enzyme to catalyze the transformation and would evade the need for the remainder of the core sequence to be constant.

We had previously shown that PapB is capable of cross-linking peptides where the Cys and Asp residues are adjacent, as well as those separated by up to six residues.[35] This suggests a model for recognition of the substrate where the active site recognizes the thiol and carboxylate moieties of the substrate only and that the remainder of the substrate, apart from the leader sequence, does not serve a role in recognition. This was further underscored by the ability to replace even the Cys and the Asp residues with D-amino acids and generate thioether cross-links in those substrates. In this report, we focused on the donor and acceptor residues and demonstrated that PapB accepts thiol and carboxylate containing side chains with

https://doi.org/10.1021/acsbiomedchemau.3c00043
ACS Bio Med Chem Au 2023, 3, 480−493

branches as well as extensions of the side chains in the hCys or hGlu examples. Additionally, we can directly replace the D23 carboxylate moiety with a bioisosteric tetrazole moiety, which may prove to exhibit more favorable pharmacological properties in future applications.

The ability to introduce cross-links in peptides containing hGlu led to the studies with unsaturated analogs of the amino acid. Both the *E*- and *Z*-forms of the substrates undergo cross-linking to dAdo. Presumably, reductive cleavage of SAM generates dAdo• in reactive proximity to the olefinic carbon of the substrate, leading to radical addition to form an intermediate, which is quenched in the case of EneA. With the diastereomeric ZneA substrate, however, a fraction of the radical intermediate is quenched by cross-linking with the Cys residue. The cross-linking of dAdo with alternate substrates has been observed in several other rSAM enzymes.[56−59] The most interesting observation here is the cross-linking to the Cys residue, which is specific to the ZneA. Together with the data with the Me-Asp variants that show a clear preference for abstraction of the *Pro-S* hydrogen, these results provide insights into the arrangement of the Cys and SAM relative to the carboxylate-containing peptide residue in the active site of the protein.

While we do not have an X-ray crystal structure of PapB yet, we were able to generate a model using Robetta (https://robetta.bakerlab.org/)[60] as shown in Figure 6. The predicted structure was aligned against a known thioether-forming rSAM RiPP homolog (CteB: 5WGG, Chain A).[21] The Fe-S clusters and SAM cofactor can be readily modeled into PapB based on their location in CteB. Further, a truncated and energy minimized version of the peptide can be docked with constraints based on known interaction of auxiliary cluster 1 (AC1) with the thiolate side chain.[42] This model predicts that the carboxylate moiety of the msPapA peptide interacts with H377 and R378 of PapB. Both residues are highly conserved in characterized and putative thioether-forming rSAM RiPP maturases. Interestingly, the *Pro-S* hydrogen at the carbon atom that is α to the carboxylate occupies a position that is proximal to the site where dAdo• would be generated in this model. If the *Pro-S* hydrogen is replaced with a methyl group, one can see that it would clash with SAM. Indeed, consistent with this constraint, (2*S*,3*R*)Me-Asp is readily turned over by PapB and (2*S*,3*S*)Me-Asp is not—presumably because in the (2*S*,3*S*)Me-Asp diastereomer, the methyl group may hinder binding and reactivity. The studies with the EneA and ZneA peptides complement this result. The dAdo• could add either α or β to the carboxylate. In the case of addition β to the carboxylate, the resulting intermediate would generate a radical α to the carboxylate, whose carbon would be appropriately positioned for thioether cross-link formation. The small quantities of thioether cross-linked ZneA that is not in a dAdo-adduct could result from abstraction of the allylic Cβ-H and subsequent reaction of the resonance-stabilized radical at either the Cδ or Cβ positions to form the thioether. We did not explore the source of this cross-linked product and could not determine the regiochemistry of the adducts because of limited sample quantities, partly because the reaction is single turnover in nature. Nevertheless, the studies with these substrate analogs provide significant clues about the arrangement of the substrate in the active site and will drive future work aimed at understanding additional elements of specificity, particularly those relating to the carboxylate-containing residue partner.

The results presented in this study demonstrate the remarkable substrate tolerance of PapB and underscore the potential to utilize rSAM RiPP maturases to design macrocyclic peptides with thioether cross-links. Indeed, without any directed evolution of any kind, we have already used PapB to synthesize an analog of octreotide,[35] which is a clinically used somatostatin inhibitor. In the context of future peptide therapeutic development, our results that demonstrate the flexibility of PapB to cross-link substrates with variable amino acids that span the space between donor/acceptor amino acids are critical. In addition, many peptide hormone receptors are highly sensitive to the size of the macrocycle—one such example is oxytocin. Altering the active core macrocycle of oxytocin from the naturally occurring 20 to 19 or 21 completely abolishes activity.[61] Our results with the extended side chains on the thiol- or carboxylate-containing side chain allows for explicit control of the peptide macrocycle ring size. Future studies on PapB will focus on additional aspects of the specificity of this remarkable enzyme in efforts to develop a model system for generalizable synthesis of thioether containing peptides that have the potential to replace disulfides and provide a facile mechanism for peptide stapling in peptide-based therapeutics and beyond.

MATERIALS AND METHODS

Expression and Purification of PapB

PapB was overexpressed and purified as previously described.[35] This procedure yields untagged PapB and includes several significant changes, including several nickel steps, TEV cleavage, and size exclusion relative to the methods published by others.[37]

Synthesis and Purification of msPapA and Variants

PapA peptides were synthesized on a Chorus peptide synthesizer (Protein Technologies Inc.). The syntheses used standard Fmoc chemistry processes and were carried out on a 0.025 mmol scale. All natural Fmoc amino acids were purchased from Protein Technologies Inc. Unnatural amino acids used in this work include Fmoc Pen(Trt)-OH (Sigma, # 670642), (2*S*,3*R*)-4-(tert-butoxy)-2-({[(9*H*-fluoren-9-yl)methoxy]carbonyl}amino)-3-methyl-4-oxobutanoic acid (Enamine # EN300-26619734), (2*S*,3*R*)-4-(tert-butoxy)-2-({[(9*H*-fluoren-9-yl)methoxy]carbonyl}amino)-3-methyl-4-oxobutanoic acid (Enamine # EN300-26619734), Fmoc D-Phe-OH (aapptec, #AFF201), Fmoc D-Lys(BOC)-OH (aapptec, #AFK205), Fmoc-hCys(Trt)-OH (Sigma, #8522660001), Fmoc-hGlu(OtBu)-OH (Sigma, #8523080001), (R)-2-(Fmoc-amino)-3-(2H-tetrazol-5-yl)-propanoic acid (1ClickChemistry, #4C92536), (E)-5-aminohex-2-enedioic acid (EneA, see Figures S35−S41) and (Z)-5-aminohex-2-enedioic acid (ZneA, see Figures S35−S41). 2-Cholorotrityl resin (ChemPep, #150301) was used for all syntheses.

The resin (150 mg) was placed in a 50 mL fritted filter chromatography tube and washed three times with 5 mL of dimethylformamide (DMF) and three times with dichloromethane (DCM). Fmoc-Ala-OH (9.3 mg, ∼0.2 mmol/g resin) was dissolved in 1 mL of 1:1 DCM:DMF along with 0.15 mmol of diisopropylethylamine (DIPEA). The chromatography tube was capped, and the solution was added to the resin. The mixture was gently shaken for 1 h. The Fmoc-Ala/DIPEA solution was then removed by uncapping the chromatography tube. The resin was then washed with three 5 mL aliquots of DCM. Any remaining uncapped sites on the resin were capped by washing with 20 mL of 17:2:1 DCM:methanol:DIPEA. The resin was then washed three times with 5 mL of DCM and three times with 5 mL of DMF and transferred to the reaction vessel.

All natural Fmoc-amino acids (0.15 mmol, 6 equivalents) were coupled by *in situ* activation with N-[(dimethylamino)-1*H*-1,2,3-triazo4,5-b]pyridin-1-ylmethylene]-*N*-methylmethanaminium hexafluorophosphate-*N*-oxide (HATU) (0.15 mmol, 6 equivalents; P3bioSystems, #31006) in 0.6 M *N*-methylmorpholine. Standard

https://doi.org/10.1021/acsbiomedchemau.3c00043
ACS Bio Med Chem Au 2023, 3, 480−493

elongation procedure are as follows: (1) 2 mL of DMF top wash; (2) 2 mL of 20% piperidine in DMF, 3 min incubation time with shaking and N_2 gas, repeated twice; (3) 2 mL of DMF top wash, repeated six times; (4) addition of the amino acid building block, HATU activator, and *N*-methylmorpholine, 7 min incubation time with shaking and N_2 gas; (5) 2 mL of DMF top wash, repeated 6 times. Unnatural amino acids followed the same elongation procedure but utilized one-shot amino acid additions. The amino acid (35 mg) was dissolved in 1 mL of DMF, and entire contents of the dissolved amino acid were added to the reaction vessel during the amino acid building block step. The N-terminal amino acid of each peptide underwent an additional round of deprotection in 20% piperidine after coupling to remove the N-terminal Fmoc group.

The peptide was cleaved from the resin, and side chain protecting groups were removed by adding 5 mL of a cleavage solution containing 87.5% (v/v) TFA, 5% (v/v) thioanisole, 3% (v/v) ethane dithiol, 2.5% (v/v) triisopropylsilane, and 2% (v/v) anisole followed by stirring for 1 h at 40 °C. The cleavage solution was filtered through a fritted 50 mL chromatography column into 30 mL of ice-cold diethyl ether to precipitate the peptide. The resulting solution was then stored on ice for 10 min to further aggregate the peptide. The precipitated peptide was collected by filtration through a Büchner funnel with vacuum. The peptide that collected over the filter was dried for 20 min before being washed with 50 mL of ice-cold diethyl ether. After drying for an additional 20 min, the dried peptide pellet was transferred to a 50 mL conical vial, dissolved in 20 mL of water, sonicated for 10 min to aid in the dissolution, flash frozen in liquid N_2, and lyophilized.

The peptides were purified on a Phenomenex Jupiter C12 or C18 preparative column (21.2 mm × 250 mm, 5 μm particle size, 300 Å pore size) attached to an Ultimate 3000 HPLC with a diode array detector. Peptides containing either an N-terminal Trp or an internal TEV protease recognition sequence were purified with the C12 column, and all others were purified with a C18 column. Buffer A contained 0.1% trifluoroacetic acid (TFA, HPLC grade) in nanopure water and buffer B contained 0.1% TFA (HPLC Grade) in acetonitrile (HPLC grade). The flow rate of the separation was 4 mL/min. A linear gradient of buffer A from 88% to 60% over 65 min was used in all scenarios. With these conditions, every peptide elutes between 44 and 49 min. Fractions were analyzed by HPLC-MS using a Vanquish UHPLC with a diode array detector connected to a Q-Exactive mass spectrometer fitted with a Hypersil GOLD C4 or C18 column (2.1 mm × 150 mm, 1.9 μm particle size). For the fraction analysis, peptides containing a C-terminal Trp or an internal TEV protease recognition site were analyzed on the C4 column, whereas a C18 column was used with all others. Separations were carried out at 0.2 mL/min. The HPLC-MS program for peptide fractions used buffer A containing Optima water (Fisher)/0.1% (v/v) Optima trifluoroacetic acid (TFA) (Fisher) and buffer B containing LC-MS Optima acetonitrile (Fisher)/0.1% (v/v) Optima TFA (Fisher). The 12 min separation consisted of 100% A for 3 min followed by a linear gradient of 0 to 100% B from 3 to 6 min followed with washing the column with 100% B from 6 to 9 min, and re-equilibration with 100% A from 9 to 12 min. The MS detector was operated in positive ion mode and the FT analyzer settings are as follows: 70,000 resolution, 1 microscan, and 200 ms maximum injection time. Data analysis for MS results used Xcalibur software (Thermo Fisher).

Enzymatic Reactions of msPapA Peptide and Variants with PapB

All assays occurred in a Coy Laboratories anerobic chamber with a 97% N_2/3% H_2 atmosphere at room temperature. Reactions were conducted in a 0.05 M PIPES•KOH (pH 7.4) buffer containing 300 mM KCl, 15% glycerol, 2 mM dithiothreitol (DTT), 2 mM SAM (enzymatically synthesized and purified as previously described),[18] 2 mM sodium dithionite (NaDT), 200 μM msPapA or variant (concentration determined by Trp absorbance or by dry weight), and 2 μM PapB (concentration determined by Bradford and amino acid analysis correction factor). The total assay volume for the reactions was 0.2 mL. Control reactions in the absence of PapB were also conducted. Reaction initiation occurred through the addition of PapB to a master mix that contained all other components. All reactions were quenched at 15 min unless otherwise specified. Quenching occurred through the addition of 10% of the reaction volume of 30% (w/v) trichloroacetic acid (TCA, ACS grade). All samples were centrifuged at 16,000*g* for 10 min in a microcentrifuge to pellet the precipitated PapB.

Alkylation of msPapA Variants

After the 15 min initial incubation, 50 μL of the enzymatic reaction was removed and reserved for treatment with IAM. A 500 mM stock of IAM was prepared in the dark and added to the 50 μL aliquot to reach a final concentration of 10 mM (5-fold excess over the DTT concentration). The reaction mixtures were incubated in the dark for 3 h before quenching with 5 μL of 30% (w/v) TCA. The samples were then centrifuged at 16,000*g* in a microcentrifuge to pellet the precipitated PapB.

Preparation of hCys-hGlu Cross-linked Peptide for NMR

Unreacted peptide (10 mg) was dissolved in 1 mL of reaction buffer and then centrifuged at 11,000*g* to pellet any remaining precipitate. The supernatant was divided into 10 1.5 mL Eppendorf tubes. SAM and NaDT were added to a final concentration of 2.4 and 2 mM, respectively. PapB was added to a final concentration of 5 μM, and the reaction incubated for 1 h before each tube was centrifuged for 10 min at 16,000*g*. The supernatants from the individual reactions were pooled and an additional aliquot of PapB was added to raise the concentration by an additional 5 μM. A stir bar was added, and the mixture stirred overnight. A 10 kDa centrifugal filter spin column was used to separate the peptide from PapB. A 1 mL aliquot of 90 μM TEV protease (purified as described previously)[35] was added to the resulting mixture and stirred for 4 h outside of the glovebox. Any remaining enzyme was quenched with the addition of 10% total assay volume of 30% (w/v) TCA.

Purification of the Liberated hCys-hGlu Peptide

A Phenomenex Jupiter C18 preparative column (21.2 mm × 250 mm, 5 μm particle size, 300 Å pore size) was used to purify the reacted hCys-hGlu peptide. Buffer A was 0.1% trifluoroacetic acid (TFA, HPLC grade) in nanopure water and buffer B was 0.1% TFA (HPLC Grade) in acetonitrile (ACN, HPLC grade). The separation consisted of 100% A from 0 to 10 min, a linear gradient from 100 to 80% A from 10 to 70 min, a column wash of 0% A from 10 to 85 min, and re-equilibration in 100% A from 85 to 100 min. Using this separation, the reacted peptide eluted during the dAdoH peak tail at 55−57 min. These fractions were pooled, lyophilized, resuspended in nanopure H_2O, and subjected to the same as above to reduce the contaminating dAdoH. In this second round, the peptide eluting at 56 min could be reasonably well separated from dAdoH eluting at 54 min. Fractions were analyzed using the same conditions listed in the synthesis and purification of msPapA and variants section previously discussed, using a C18 column.

Proton NMR of the Reacted and Unreacted hCys-hGlu Peptides

^{1}H-nuclear magnetic resonance (NMR) spectra were recorded on an Agilent Directdrive 500 spectrometer equipped with a high-sensitivity cold-probe or on an Agilent Directdrive 800 spectrometer. ^{1}H-NMR spectra were acquired at 500 or 800 MHz, and the chemical shifts (δ) of proton resonances were reported relative to the residual solvent peak (4.79 ppm for H_2O).

ROESY of the Reacted and Unreacted hCys-hGlu Peptides

Rotating frame Overhauser enhancement spectroscopy (ROESY) was recorded on an Agilent DirectDrive 500 spectrometer equipped with a high-sensitivity cold-probe. The following parameters were used: scans per t1 increment (nt) = 48, t1 increments (ni) = 256, relaxation delay (d1) = 1 s, spinlock mixing time (mixR) = 3 ms , spectral width (sw) = 4496.4 Hz, and complex points (np/2) = 1024. Water suppression was used in the reacted hCys-hGlu peptide using PRESAT with the transmitter offset and presaturation frequency set to 4.65 ppm.

https://doi.org/10.1021/acsbiomedchemau.3c00043
ACS Bio Med Chem Au 2023, 3, 480−493

Collision-Induced Dissociation (CID) Fragmentation of msPapA Variants

After quenching enzymatic reactions with TCA and centrifugation to remove precipitated PapB, a 100 μL aliquot was desalted using C18 ZipTips (Millipore, #ZTC18S) following the manufacturer's protocols. The resulting mixture was diluted to 200 μL using a 50:50 mixture of H_2O:acetonitrile with 0.1% Optima TFA (Fisher). Using direct injection, the analyzer was first tuned to the mass of each msPapA variant. The $z = 3$ charge state corresponding to each variant was isolated in the CID cell using an isolation width of ± 2 m/z, 0.1 ms activation time, a resolution of 70,000, and fragmented using a Normalized Collision Energy (NCE) of 25. The fragments were analyzed using mMass software.

Quantifying Turnover of Peptides by PapB

In this study, the extent of cross-linking is determined by comparisons of the intensity of the monoisotopic peak of the cross-linked species to the peak in the envelope that has contributions from the monoisotopic peak of the unmodified peptide (see Figure S49 for simulated envelopes corresponding to 0%−100% turnover).

■ ASSOCIATED CONTENT

Supporting Information

The Supporting Information is available free of charge at https://pubs.acs.org/doi/10.1021/acsbiomedchemau.3c00043.

Detailed synthetic methods for the unnatural amino acids used, gel of the purified protein, expected and observed monoisotopic masses of the processed and unprocessed peptides, mass spectrometry data for peptides treated with IAM, tandem mass spectrometry data, and the 1D and 2D NMR data (PDF)

■ AUTHOR INFORMATION

Corresponding Author

Vahe Bandarian − *Department of Chemistry, University of Utah, Salt Lake City, Utah 84112, United States;* orcid.org/0000-0003-2302-0277; Email: vahe@chem.utah.edu

Authors

Karsten A. S. Eastman − *Department of Chemistry, University of Utah, Salt Lake City, Utah 84112, United States;* orcid.org/0000-0002-2754-4222

Marcus C. Mifflin − *Department of Chemistry, University of Utah, Salt Lake City, Utah 84112, United States;* orcid.org/0000-0002-5283-9663

Paul F. Oblad − *Department of Chemistry, University of Utah, Salt Lake City, Utah 84112, United States*

Andrew G. Roberts − *Department of Chemistry, University of Utah, Salt Lake City, Utah 84112, United States;* orcid.org/0000-0002-2221-534X

Complete contact information is available at: https://pubs.acs.org/10.1021/acsbiomedchemau.3c00043

Author Contributions

K.A.S.E. expressed, purified, and characterized the enzyme and peptide substrates and performed all assays, mass spectrometric analysis, and NMR analysis. M.C.M. synthesized, purified, and characterized the proEneA and proZneA peptides. P.O. performed the 2D-NMR experiments with K.A.S.E. K.A.S.E. and V.B. wrote the manuscript with contributions from all authors. V.B. and A.G.R. supervised the research. All authors have given approval to the final version of the manuscript. CRediT: **Karsten A. S. Eastman** conceptualization (lead), data curation (lead), formal analysis (lead), funding acquisition (supporting), investigation (lead), methodology (lead), validation (lead), visualization (lead), writing-original draft (lead), writing-review & editing (equal); **Marcus C. Mifflin** conceptualization (supporting), data curation (supporting), formal analysis (supporting), investigation (supporting), methodology (supporting); **Paul F. Oblad** formal analysis (supporting); **Andrew G. Roberts** conceptualization (supporting), formal analysis (supporting), investigation (supporting), methodology (supporting), writing-review & editing (supporting); **Vahe Bandarian** conceptualization (equal), formal analysis (equal), funding acquisition (equal), investigation (equal), methodology (equal), project administration (equal), resources (equal), software (equal), supervision (equal), validation (equal), visualization (equal), writing-original draft (supporting), writing-review & editing (lead).

Notes

The authors declare the following competing financial interest(s): The work described in this manuscript has been reported to the University of Utah, which has patent interest in the findings.

■ ACKNOWLEDGMENTS

V.B. is supported by the National Institute of General Medical Sciences of the National Institutes of Health by the Grant R35-GM126956. K.A.S.E. is supported by NIH Grant T32-GM122740.

■ REFERENCES

(1) Zhang, R. K.; Chen, K.; Huang, X.; Wohlschlager, L.; Renata, H.; Arnold, F. H. Enzymatic assembly of carbon-carbon bonds via iron-catalysed sp(3) C-H functionalization. *Nature* **2019**, *565*, 67−72.

(2) Lewis, J. C.; Coelho, P. S.; Arnold, F. H. Enzymatic functionalization of carbon-hydrogen bonds. *Chem. Soc. Rev.* **2011**, *40*, 2003−2021.

(3) Craven, E. J.; Latham, J.; Shepherd, S. A.; Khan, I.; Diaz-Rodriguez, A.; Greaney, M. F.; Micklefield, J. Programmable late-stage C−H bond functionalization enabled by integration of enzymes with chemocatalysis. *Nat. Catal.* **2021**, *4*, 385−394.

(4) Reetz, M. T. Biocatalysis in organic chemistry and biotechnology: past, present, and future. *J. Am. Chem. Soc.* **2013**, *135*, 12480−12496.

(5) Faber, K.; Fessner, W. D.; Turner, N. J. Biocatalysis: Ready to master increasing complexity. *Adv. Synth. Catal.* , *361*, 2373 DOI: 10.1002/adsc.201900610.

(6) Rocha, R. A.; Speight, R. E.; Scott, C. Engineering enzyme properties for improved biocatalytic processes in batch and continuous flow. *Org. Process Res. Dev.* **2022**, *26*, 1914−1924.

(7) Oberg, N.; Precord, T. W.; Mitchell, D. A.; Gerlt, J. A. RadicalSAM.org: A resource to interpret sequence-function space and discover new radical SAM enzyme chemistry. *ACS Bio. Med. Chem. Au* **2022**, *2*, 22−35.

(8) Sofia, H. J.; Chen, G.; Hetzler, B. G.; Reyes-Spindola, J. F.; Miller, N. E. Radical SAM, a novel protein superfamily linking unresolved steps in familiar biosynthetic pathways with radical mechanisms: functional characterization using new analysis and information visualization methods. *Nucleic Acids Res.* **2001**, *29*, 1097−1106.

(9) Broderick, J. B.; Duffus, B. R.; Duschene, K. S.; Shepard, E. M. Radical S-adenosylmethionine enzymes. *Chem. Rev.* **2014**, *114*, 4229−4317.

(10) Wecksler, S. R.; Stoll, S.; Tran, H.; Magnusson, O. T.; Wu, S. P.; King, D.; Britt, R. D.; Klinman, J. P. Pyrroloquinoline quinone biogenesis: demonstration that PqqE from Klebsiella pneumoniae is a radical S-adenosyl-L-methionine enzyme. *Biochemistry* **2009**, *48*, 10151.
(11) Hover, B. M.; Tonthat, N. K.; Schumacher, M. A.; Yokoyama, K. Mechanism of pyranopterin ring formation in molybdenum cofactor biosynthesis. *Proc. Natl. Acad. Sci. U. S. A.* **2015**, *112*, 6347−6352.
(12) Ebrahimi, K. H.; Howie, D.; Rowbotham, J. S.; McCullagh, J.; Armstrong, F. A.; James, W. S. Viperin, through its radical-SAM activity, depletes cellular nucleotide pools and interferes with mitochondrial metabolism to inhibit viral replication. *FEBS Lett.* **2020**, *594*, 1624−1630.
(13) McLaughlin, M. I.; Lanz, N. D.; Goldman, P. J.; Lee, K. H.; Booker, S. J.; Drennan, C. L. Crystallographic snapshots of sulfur insertion by lipoyl synthase. *Proc. Natl. Acad. Sci. U. S. A.* **2016**, *113*, 9446−9450.
(14) Berkovitch, F.; Nicolet, Y.; Wan, J. T.; Jarrett, J. T.; Drennan, C. L. Crystal structure of biotin synthase, an S-adenosylmethionine-dependent radical enzyme. *Science* **2004**, *303*, 76−79.
(15) Chen, D.; Ruzicka, F. J.; Frey, P. A. A novel lysine 2,3-aminomutase encoded by the yodO gene of bacillus subtilis: characterization and the observation of organic radical intermediates. *Biochem. J.* **2000**, *348*, 539−549.
(16) Chandor, A.; Berteau, O.; Douki, T.; Gasparutto, D.; Sanakis, Y.; Ollagnier-de-Choudens, S.; Atta, M.; Fontecave, M. Dinucleotide spore photoproduct, a minimal substrate of the DNA repair spore photoproduct lyase enzyme from Bacillus subtilis. *J. Biol. Chem.* **2006**, *281*, 26922−26931.
(17) Benjdia, A.; Heil, K.; Barends, T. R. M.; Carell, T.; Schlichting, I. Structural insights into recognition and repair of UV-DNA damage by Spore Photoproduct Lyase, a radical SAM enzyme. *Nucleic Acids Res.* **2012**, *40*, 9308−9318.
(18) Young, A. P.; Bandarian, V. TYW1: A radical SAM enzyme involved in the biosynthesis of wybutosine bases. *Methods Enzymol.* **2018**, *606*, 119−153.
(19) Hernández, H. L.; Pierrel, F.; Elleingand, E.; García-Serres, R.; Huynh, B. H.; Johnson, M. K.; Fontecave, M.; Atta, M. MiaB, a bifunctional radical-S-adenosylmethionine enzyme involved in the thiolation and methylation of tRNA, contains two essential [4Fe-4S] clusters. *Biochemistry* **2007**, *46*, 5140−5147.
(20) Esakova, O. A.; Grove, T. L.; Yennawar, N. H.; Arcinas, A. J.; Wang, B.; Krebs, C.; Almo, S. C.; Booker, S. J. Structural basis for tRNA methylthiolation by the radical SAM enzyme MiaB. *Nature* **2021**, *597*, 566−570.
(21) Grove, T. L.; Himes, P. M.; Hwang, S.; Yumerefendi, H.; Bonanno, J. B.; Kuhlman, B.; Almo, S. C.; Bowers, A. B. Structural Insights into Thioether Bond Formation in the Biosynthesis of Sactipeptides. *J. Am. Chem. Soc.* **2017**, *139*, 11734.
(22) Grell, T. A. J.; Kincannon, W. M.; Bruender, N. A.; Blaesi, E. J.; Krebs, C.; Bandarian, V.; Drennan, C. L. Structural and spectroscopic analyses of the sporulation killing factor biosynthetic enzyme SkfB, a bacterial AdoMet radical sactisynthase. *J. Biol. Chem.* **2018**, *293*, 17349−17361.
(23) Balty, C.; Guillot, A.; Fradale, L.; Brewee, C.; Boulay, M.; Kubiak, X.; Benjdia, A.; Berteau, O. Ruminococcin C, an anti-clostridial sactipeptide produced by a prominent member of the human microbiota Ruminococcus gnavus. *J. Biol. Chem.* **2019**, *294*, 14512−14525.
(24) Schramma, K. R.; Bushin, L. B.; Seyedsayamdost, M. R. Structure and biosynthesis of a macrocyclic peptide containing an unprecedented lysine-to-tryptophan cross-link. *Nat. Chem.* **2015**, *7*, 431−437.
(25) Khaliullin, B.; Aggarwal, P.; Bubas, M.; Eaton, G. R.; Eaton, S. S.; Latham, J. A. Mycofactocin biosynthesis: modification of the peptide MftA by the radical S-adenosylmethionine protein MftC. *FEBS Lett.* **2016**, *590*, 2538−2548.
(26) Bruender, N. A.; Wilcoxen, J.; Britt, R. D.; Bandarian, V. Biochemical and spectroscopic characterization of a radical *S*-adenosyl-$_L$-methionine enzyme involved in the formation of a peptide thioether cross-link. *Biochemistry* **2016**, *55*, 2122−2134.
(27) Popp, P. F.; Friebel, L.; Benjdia, A.; Guillot, A.; Berteau, O.; Mascher, T. The epipeptide biosynthesis locus epeXEPAB is widely distributed in firmicutes and triggers intrinsic cell envelope stress. *Microb. Physiol.* **2021**, *31*, 306−318.
(28) Crain, A. V.; Broderick, J. B. Pyruvate formate-lyase and its activation by pyruvate formate-lyase activating enzyme. *J. Biol. Chem.* **2014**, *289*, 5723−5729.
(29) Shisler, K. A.; Broderick, J. B. Glycyl radical activating enzymes: structure, mechanism, and substrate interactions. *Arch. Biochem. Biophys.* **2014**, *546*, 64−71.
(30) Benjdia, A.; Leprince, J.; Guillot, A.; Vaudry, H.; Rabot, S.; Berteau, O. Anaerobic sulfatase-maturating enzymes: radical SAM enzymes able to catalyze in vitro sulfatase post-translational modification. *J. Am. Chem. Soc.* **2007**, *129*, 3462−3463.
(31) King, A. M.; Anderson, D. A.; Glassey, E.; Segall-Shapiro, T. H.; Zhang, Z.; Niquille, D. L.; Embree, A. C.; Pratt, K.; Williams, T. L.; Gordon, D. B.; et al. Selection for constrained peptides that bind to a single target protein. *Nat. Commun.* **2021**, *12*, 6343.
(32) Himes, P. M.; Allen, S. E.; Hwang, S.; Bowers, A. A. Production of sactipeptides in Escherichia coli: Probing the substrate promiscuity of subtilosin A biosynthesis. *ACS Chem. Biol.* **2016**, *11*, 1737−1744.
(33) Vagstad, A. L.; Kuranaga, T.; Püntener, S.; Pattabiraman, V. R.; Bode, J. W.; Piel, J. Introduction of D-amino acids in minimalistic peptide substrates by an S-adenosyl-L-methionine radical epimerase. *Angew. Chem., Int. Ed.* **2019**, *58*, 2246−2250.
(34) Korneli, M.; Fuchs, S. W.; Felder, K.; Ernst, C.; Zinsli, L. V.; Piel, J. Promiscuous Installation of D-amino acids in gene-encoded peptides. *ACS Synth. Biol.* **2021**, *10*, 236−242.
(35) Eastman, K. A. S.; Kincannon, W. M.; Bandarian, V. Leveraging substrate promiscuity of a radical S-adenosyl-L-methionine RiPP maturase toward intramolecular peptide cross-linking applications. *ACS Cent. Sci.* **2022**, *8*, 1209−1217.
(36) Hudson, G. A.; Burkhart, B. J.; DiCaprio, A. J.; Schwalen, C. J.; Kille, B.; Pogorelov, T. V.; Mitchell, D. A. Bioinformatic mapping of radical *S*-adenosylmethionine-dependent ribosomally synthesized and post-translationally modified peptides identifies new Cα, Cβ, and Cγ-linked thioether-containing peptides. *J. Am. Chem. Soc.* **2019**, *141*, 8228−8238.
(37) Precord, T. W.; Mahanta, N.; Mitchell, D. A. Reconstitution and substrate specificity of the thioether-forming radical S-adenosylmethionine enzyme in freyrasin biosynthesis. *ACS Chem. Biol.* **2019**, *14*, 1981−1989.
(38) Grell, T. A. J.; Goldman, P. J.; Drennan, C. L. SPASM and twitch domains in S-adenosylmethionine (SAM) radical enzymes. *J. Biol. Chem.* **2015**, *290*, 3964−3971.
(39) Davis, K. M.; Schramma, K. R.; Hansen, W. A.; Bacik, J. P.; Khare, S. D.; Seyedsayamdost, M. R.; Ando, N. Structures of the peptide-modifying radical SAM enzyme SuiB elucidate the basis of substrate recognition. *Proc. Natl. Acad. Sci. U. S. A.* **2017**, *114*, 10420−10425.
(40) Dowling, D. P.; Bruender, N. A.; Young, A. P.; McCarty, R. M.; Bandarian, V.; Drennan, C. L. Radical SAM enzyme QueE defines a new minimal core fold and metal-dependent mechanism. *Nat. Chem. Biol.* **2014**, *10*, 106−112.
(41) Sarkar, S.; Gu, W.; Schmidt, E. W. Expanding the chemical space of synthetic cyclic peptides using a promiscuous macrocyclase from prenylagaramide biosynthesis. *ACS Catal.* **2020**, *10*, 7146−7153.
(42) Rush, K. W.; Eastman, K. A. S.; Kincannon, W. M.; Blackburn, N. J.; Bandarian, V. Peptide selenocysteine substitutions reveal direct substrate-enzyme interactions at auxiliary clusters in radical *S*-adenosyl-$_L$-methionine maturases. *J. Am. Chem. Soc.* **2023**, *145*, 10167−10177.
(43) Zou, Y.; Liu, L.; Liu, J.; Liu, G. Bioisosteres in drug discovery: focus on tetrazole. *Future Med. Chem.* **2020**, *12*, 91−93.

https://doi.org/10.1021/acsbiomedchemau.3c00043
ACS Bio Med Chem Au 2023, 3, 480−493

(44) Ballatore, C.; Huryn, D. M.; Smith, A. B. I. I. I. Carboxylic acid (bio)isosteres in drug design. *ChemMedChem* **2013**, *8*, 385−395.
(45) Lassalas, P.; Gay, B.; Lasfargeas, C.; James, M. J.; Tran, V.; Vijayendran, K. G.; Brunden, K. R.; Kozlowski, M. C.; Thomas, C. J.; Smith, A. B. I. I. I.; et al. Structure property relationships of carboxylic acid isosteres. *J. Med. Chem.* **2016**, *59*, 3183−3203.
(46) Darnell, M.; Weidolf, L. Metabolism of xenobiotic carboxylic acids: focus on coenzyme A conjugation, reactivity, and interference with lipid metabolism. *Chem. Res. Toxicol.* **2013**, *26*, 1139−1155.
(47) Subramanian, V.; Knight, J. S.; Parelkar, S.; Anguish, L.; Coonrod, S. A.; Kaplan, M. J.; Thompson, P. R. Design, synthesis, and biological evaluation of tetrazole analogs of Cl-amidine as protein arginine deiminase inhibitors. *J. Med. Chem.* **2015**, *58*, 1337−1344.
(48) Lamie, P. F.; Philoppes, J. N.; Azouz, A. A.; Safwat, N. M. Novel tetrazole and cyanamide derivatives as inhibitors of cyclo-oxygenase-2 enzyme: design, synthesis, anti-inflammatory evaluation, ulcerogenic liability and docking study. *J. Enzyme Inhib. Med. Chem.* **2017**, *32*, 805−820.
(49) Noda, K.; Saad, Y.; Kinoshita, A.; Boyle, T. P.; Graham, R. M.; Husain, A.; Karnik, S. S. Tetrazole and carboxylate groups of angiotensin receptor antagonists bind to the same subsite by different mechanisms. *J. Biol. Chem.* **1995**, *270*, 2284−2289.
(50) Gao, F.; Xiao, J.; Huang, G. Current scenario of tetrazole hybrids for antibacterial activity. *Eur. J. Med. Chem.* **2019**, *184*, No. 111744.
(51) Nolen, E. G.; Kurish, A. J.; Potter, J. M.; Donahue, L. A.; Orlando, M. D. Stereoselective synthesis of alpha-C-glucosyl serine and alanine via a cross-metathesis/cyclization strategy. *Org. Lett.* **2005**, *7*, 3383−3386.
(52) Wang, Y.; Xue, P.; Cao, M.; Yu, T.; Lane, S. T.; Zhao, H. Directed Evolution: Methodologies and Applications. *Chem. Rev.* **2021**, *121*, 12384−12444.
(53) Otten, R.; Pádua, R. A. P.; Bunzel, H. A.; Nguyen, V.; Pitsawong, W.; Patterson, M.; Sui, S.; Perry, S. L.; Cohen, A. E.; Hilvert, D.; et al. How directed evolution reshapes the energy landscape in an enzyme to boost catalysis. *Science* **2020**, *370*, 1442−1446.
(54) Nirantar, S. R. Directed evolution methods for enzyme engineering. *Molecules* **2021**, *26*, 5599.
(55) Broom, A.; Rakotoharisoa, R. V.; Thompson, M. C.; Zarifi, N.; Nguyen, E.; Mukhametzhanov, N.; Liu, L.; Fraser, J. S.; Chica, R. A. Ensemble-based enzyme design can recapitulate the effects of laboratory directed evolution in silico. *Nat. Commun.* **2020**, *11*, 4808.
(56) Wilcoxen, J.; Bruender, N. A.; Bandarian, V.; Britt, R. D. A radical intermediate in Bacillus subtilis QueE during turnover with the substrate analogue 6-Carboxypterin. *J. Am. Chem. Soc.* **2018**, *140*, 1753−1759.
(57) Ji, X.; Li, Y.; Xie, L.; Lu, H.; Ding, W.; Zhang, Q. Expanding radical SAM chemistry by using radical addition reactions and SAM analogues. *Angew. Chem., Int. Ed.* **2016**, *55*, 11845−11848.
(58) Lee, Y. H.; Yeh, Y. C.; Fan, P. H.; Zhong, A.; Ruszczycky, M. W.; Liu, H. W. Changing fates of the substrate radicals generated in the active sites of the B(12)-dependent radical SAM enzymes OxsB and AlsB. *J. Am. Chem. Soc.* **2023**, *145*, 3656−3664.
(59) Ji, X.; Mandalapu, D.; Cheng, J.; Ding, W.; Zhang, Q. Expanding the chemistry of the class C radical SAM methyltransferase NosN by using an Allyl analogue of SAM. *Angew. Chem., Int. Ed.* **2018**, *57*, 6601−6604.
(60) Du, Z.; Su, H.; Wang, W.; Ye, L.; Wei, H.; Peng, Z.; Anishchenko, I.; Baker, D.; Yang, J. The trRosetta server for fast and accurate protein structure prediction. *Nat. Protoc.* **2021**, *16*, 5634−5651.
(61) Muttenthaler, M.; Andersson, A.; de Araujo, A. D.; Dekan, Z.; Lewis, R. J.; Alewood, P. F. Modulating oxytocin activity and plasma stability by disulfide bond engineering. *J. Med. Chem.* **2010**, *53*, 8585−8596.

https://doi.org/10.1021/acsbiomedchemau.3c00043
ACS Bio Med Chem Au 2023, 3, 480−493